Biomedical Signal Processing and Control 40 (2018) 275–285

Contents lists available at ScienceDirect

Biomedical Signal Processing and Control

journal homepage: www.elsevier.com/locate/bspc

A robust unsupervised epileptic seizure detection methodology to accelerate large EEG database evaluation

Kostas M. Tsiouris [a,d], Sofia Markoula [b], Spiros Konitsiotis [c], Dimitrios. D. Koutsouris [a], Dimitrios I. Fotiadis [d,e,*]

[a] Biomedical Engineering Laboratory, School of Electrical and Computer Engineering, National Technical University of Athens, GR15773, Athens, Greece
[b] University Hospital of Ioannina, GR45110, Ioannina, Greece
[c] Department of Neurology, Medical School, University of Ioannina, GR45110, Ioannina, Greece
[d] Unit of Medical Technology and Intelligent Information Systems, Department of Materials Science and Engineering, University of Ioannina, GR45110, Ioannina, Greece
[e] Department of Biomedical Research, Institute of Molecular Biology and Biotechnology, FORTH, University of Ioannina, GR45110, Ioannina, Greece

ARTICLE INFO

Article history:
Received 31 March 2017
Received in revised form 15 September 2017
Accepted 30 September 2017
Available online 12 October 2017

Keywords:
EEG
Epilepsy
Unsupervised seizure detection
Medical knowledge
Time-Frequency analysis

ABSTRACT

In this work an unsupervised methodology for the detection of epileptic seizures in long-term EEG recordings is presented. The design of the methodology exploits the available medical knowledge to tackle the lack of training data using a simple rule-based seizure detection logic, avoiding complex decision making systems, training and empirical thresholds. The Short-Time Fourier Transform is initially applied to extract the EEG signal energy distribution over the delta (<4 Hz), theta (4–7 Hz) and alpha (8–13 Hz) frequency bands. A set of four novel seizure detection conditions is proposed to isolate EEG segments with increased potential of containing ictal activity, by identifying segments where the EEG signal energy is intensively accumulated among the three fundamental frequency rhythms. A set of candidate seizure segments is extracted based on the intensity of the accumulated EEG activity per seizure detection condition. The clinician has to visually inspect only the extracted segments instead of the entire duration of the patient's EEG recordings to speed up the annotation process. The results from the evaluation with 24 cases of long-term EEG recordings, suggest that the proposed methodology can reach on average up to 89% of seizure detection sensitivity, by automatically rejecting 95% of the total patient's EEG recordings as non-ictal, without requiring any *apriori* data knowledge.

1. Introduction

Epilepsy is a neurological condition expressed with the occurrence of seizures that alter the normal electrical activity between the brain's neurons, leading to various clinical manifestations depending on the affected area of the brain. As much as 50 million people are estimated to suffer from epilepsy, 30% of whom do not respond to treatment with anti-epileptic medication (WHO, 2012). The electroencephalogram (EEG) is used to capture the electrical activity of the brain. It is considered the golden standard for epilepsy diagnosis and is the most cost effective means for long-term monitoring of patients with any suspected or diagnosed epileptic syndromes [1]. Nowadays, continuous recording of EEG signals, for up to several days, is a very common practice due to cost reduction in data storage. However, this practice yields extensive volumes of EEG data that have to be carefully inspected for signs of ictal activity in order to isolate seizure segments for further analysis. Visual inspection of large volumes of EEG signals has proven to be an extremely time consuming and tedious task even for domain experts. In the direction of relieving part of the annotation effort and automating the detection of epileptic seizures, machine learning techniques and unsupervised methodologies have been introduced in the analysis of EEG signals.

Over the past few years, many supervised methodologies have been proposed for the detection of epileptic seizures, highlighting the need for developing tools for faster annotation of large volumes of EEG data even in non-seizure detection applications [2,3]. The vast majority of the available machine learning techniques have been used in seizure detection, ranging from the more simplistic ones such as the k-nearest neighbors algorithm (k-NN) [4], to the very popular Support Vector Machines (SVMs) [5] and the more

* Corresponding author at: Unit of Medical Technology and Intelligent Information Systems, Department of Materials Science and Engineering, University of Ioannina, GR45110, Ioannina, Greece.
E-mail address: fotiadis@cc.uoi.gr (D.I. Fotiadis).

https://doi.org/10.1016/j.bspc.2017.09.029
1746-8094/

computationally demanding neural networks (NNs) [6,7]. The classification process was often complemented with the addition of clustering techniques, which exploit the EEG signal's variations to extract clusters of similar activity in an attempt to increase the classifier's seizure detection performance [8,9]. Besides clustering and classification, rule-based seizure detection methodologies have also been studied as an alternative solution. In these methodologies, a wide variety of EEG signal behavior criteria and/or threshold-crossing parameters have been combined to declare the occurrence of ictal activity when triggered [10–13]. A set of training EEG data was required to extract the seizure detection criteria and to fine tune the seizure detection thresholds, prior to the evaluation with the testing subset. Furthermore, seizure detection methodologies based on fuzzy rule-based decision-making systems have been tested as well [14], showing great potential in mimicking the EEG expert's reasoning in declaring ictal activity.

In an attempt to demonstrate the applicability of machine learning techniques in everyday clinical practice, researchers have also introduced external validation of their methodologies with out of sample EEG data. In most cases a classifier (i.e. SVM, k-NN, Bayesian and Neural Networks) was trained using a set of EEG recordings from a subgroup of the available patients and was then validated using the rest of the EEG dataset from the remaining patients [15–17]. The classifier's ability to adapt to new patients was evaluated by measuring its seizure detection performance on the latter. In more recent publications, researchers have also investigated the potential gains from using a much wider set of features when training their classifiers, in order to address their impact in classification performance [18,19]. In other such systems, instead of focusing on classification techniques, the researchers used the EEG recordings from the training group to extract seizure detection criteria and/or adjust feature-related detection thresholds, in an attempt to optimize their methodologies for better out of sample detection performance [20–22].

Compared to unsupervised methodologies, the main drawback of using machine learning techniques such as the above, is that they require pre-annotated EEG data or some kind of *apriori* information during the training process. On the other hand, the challenge in using unsupervised techniques is to find a universal methodology that would adapt to multiple patients. The possibility of developing an unsupervised seizure detection methodology that attributes variations in the EEG signals to the occurrence of epileptic seizures has been under investigation over the past few years. Researchers have initially shown that ictal EEG activity caused specific ictal EEG signal manifestations that were uncommon during the interictal state or further away from the epileptogenic zone [23,24]. These works, however, examined small segments of EEG recordings (usually a seizure and a few minutes of EEG before and after) showing a proof of concept rather than a complete evaluation. Recently, Birjandtalab et al. [25] presented an unsupervised methodology for the detection of epileptic EEG activity using features extracted from spectral analysis and clustering, further enhancing the semi-automated framework set by Smart and Chen [26]. These methodologies were evaluated using the same EEG database as in this work, but only a few of the available cases and only seizure adjacent EEG segments. However, despite the limited dataset, the results provided significant evidence for the effectiveness of EEG spectral analysis in identifying ictal activity in an unsupervised manner.

In this work, a methodology is proposed to detect and isolate segments with epileptic EEG activity in a completely unsupervised manner, based on four novel seizure detection conditions (Section 2.3). Using the proposed conditions, the EEG segments that are more likely to contain epileptic activity are automatically isolated for visual inspection and validation without requiring any user intervention, *apriori* information about the patient or any EEG data for training. The advantage of the proposed conditions is that they have been formulated combining the available medical knowledge and understanding regarding the different expressions of ictal activity in EEG signals and previous literature findings of EEG signal processing techniques in the automated seizure detection field. Our primary goal is to provide a system that offers high seizure detection rates while drastically reducing the time required for the annotation of long-term EEG recordings. Furthermore, to the best of our knowledge, this is the first time that an unsupervised seizure detection methodology has been evaluated using such an extensive volume of EEG data from a public database, consisting of about 983 h of scalp EEG recordings and 198 seizures [27].

2. Materials and methods

2.1. EEG dataset

The CHB-MIT EEG database contains scalp EEG signals from 23 subjects with intractable epileptic seizures (5 males, aged 3–22 years old; 17 females, aged 1.5-19 years old; 1 missing gender/age data), recorded at the Children's Hospital Boston in cooperation with the Massachusetts Institute of Technology [28]. The subjects were monitored for up to several days, following withdrawal of their anti-epileptic medication in order to isolate the epileptogenic area and evaluate the possibility of surgical intervention. In total, there are more than 980 h of raw EEG signals available, collected following the International 10–20 standard system of EEG electrode positions. The recordings were organized in 24 cases, each containing EEG data from a single subject, except cases 1 and 21 which were obtained from the same subject with a 1.5 year interval. All signals were sampled at 256 samples per second with 16-bit resolution. As changes in EEG montage were frequent within each case, the number of the available EEG signals varies, with most of the files consisting of 23 signals, while 24 and 26 signals were included in others. During the annotation phase, 198 events were identified as epileptic seizures by clinical experts who marked their electroencephalographic onset and offset after visual inspection. The contents of the CHB-MIT database are presented in full detail in Table 1. The database is available at PhysioNet.org/pn6/chbmit [27,29].

2.2. Medical knowledge background

According to the International League Against Epilepsy, ILAE, an epileptic seizure can be defined as a transient occurrence of signs and/or symptoms due to abnormal excessive or synchronous neuronal activity in the brain [30]. The EEG patterns of epileptic seizures contain one of the well-established spike, wave and spike-wave combinations and usually include dominant bursts of rhythmical activity that begin suddenly and, depending on the type of seizure, may evolve to other regions of the brain during the seizure [31]. That is why the spectral contents of the EEG signals are important for the detection of epileptic seizures. These ictal patterns are most often represented with rhythmical activity within the delta (<4 Hz), theta (4–7 Hz), alpha (8–13 Hz) and gamma (13–30 Hz) waves, or the slow component of the spike-wave complex, in seizures where such EEG activity is expressed.

The medical background is further supported by the findings of previous EEG signal processing methodologies targeting epileptic seizure detection, where the EEG activity within the 1–30 Hz frequency band, in particular, was found to be highly seizure-related [20,32–36]. Furthermore, ictal rhythmical activity is proven to be a solid indication of seizure occurrence and a more reliable way to detect such events compared to spike and/or wave symiological expressions. This is greatly depicted by the prevalence of EEG spec-

Table 1
The CHB-MIT EEG database. Gender: female (F), male (M). Duration of Recordings: total duration of available EEG recordings (interictal and ictal). Duration of Seizures: total duration of ictal activity.

Case	Gender	Age (years)	# of Seizures	Duration of Recordings (hh:mm:ss)	Duration of Seizures (min)
1	F	11	7	40:33:08	7.37
2	M	11	3	35:15:59	2.87
3	F	14	7	38:00:06	6.70
4	M	22	4	156:03:54	6.30
5	F	7	5	39:00:10	9.30
6	F	1.5	10	66:44:06	2.55
7	F	14.5	3	67:03:08	5.42
8	M	3.5	5	20:00:23	15.32
9	F	10	4	67:52:18	4.60
10	M	3	7	50:01:24	7.45
11	F	12	3	34:47:37	13.43
12	F	2	40	23:41:40	24.58
13	F	3	12	33:00:00	8.92
14	F	9	8	26:00:00	2.82
15	M	16	20	40:00:36	33.20
16	F	7	10	19:00:00	1.40
17	F	12	3	21:00:24	4.88
18	F	18	6	35:38:05	5.28
19	F	19	3	29:55:46	3.93
20	F	6	8	27:36:06	4.90
21	F	13	4	32:49:49	3.32
22	F	9	3	31:00:11	3.40
23	F	6	7	26:33:30	7.07
24	–	–	16	21:17:47	8.52
Total:			198	982:56:07	193.52

tral analysis and time-frequency applications against time domain and pattern recognition techniques in the literature [36–39]. In an attempt to make the most out of the available medical and signal processing knowledge, the proposed seizure detection methodology focuses on the analysis of the mid-low frequency range of the EEG signals using a novel set of four simple conditions to discriminate segments of ictal activity in a completely unsupervised manner.

2.3. Seizure detection conditions

Based on the existing knowledge the relative EEG energy distribution across the delta (<4Hz), theta (4–7 Hz) and alpha (8–13 Hz) frequency bands is estimated, as ictal rhythmical activity is expected to cause the accumulation of more energy over these three frequency bands. By continuously monitoring EEG energy distribution from multiple electrodes positioned around the patient's scalp, the proposed methodology can detect the occurrence of an epileptic seizure if there is a significant concentration of rhythmical activity towards a specific sub-band of the examined frequency spectrum. Thus, since the concentration of rhythmical EEG activity is attributed to a potential seizure occurrence, an EEG segment is regarded as containing ictal activity if one or more of the following conditions are met:

Condition 1. Accumulated activity over theta band (4–7 Hz) larger than delta and alpha bands.

Condition 2. Accumulated activity over alpha band (8–13 Hz) larger than delta and theta bands.

Condition 3. Accumulated activity over theta and alpha bands (4–13 Hz) larger than delta band.

Condition 4. Accumulated activity over delta and theta bands (2–7 Hz) larger than alpha band.

These conditions are kept to a generalized format in order to be as widely applicable as possible to patients with different types of epilepsy and various manifestations of ictal EEG activity. *Conditions 3* and *4*, in particular, are used to detect seizures in cases of wide spread ictal rhythmical activity which is not restricted within the frequency range of a single band. The novelty of the proposed seizure detection conditions, is the use of the relative energy distribution among the three energy bands for triggering their activation, instead of relying on predefined activation thresholds or empirical values, retaining its unsupervised privilege. When any of these conditions is activated, the respective EEG segment is regarded as candidate for containing ictal activity. The segments where the rhythmical EEG activity is more intensively and highly concentrated are the most likely to contain an epileptic seizure. The best of these EEG segments will be finally presented to the medical expert for visual inspection, making the annotation process faster and much easier as only a small fraction of the long-term recording will require manual interpretation.

2.4. EEG analysis

In order to apply the proposed seizure detection conditions, the energy contents of the three EEG frequency bands are extracted using time-frequency analysis. The Short-Time Fourier Transform (STFT) is selected for this task due to its very low computational cost, as hours of EEG signals can be transformed into a few seconds, compensating for potential underestimations compared to more complex techniques such as Wavelets and Hilbert-Huang Transform [40,41]. The EEG signal processing part of this work has been introduced in our preliminary work [42]. The first step is to ensure channel consistency across the entire duration of the examined EEG recordings of each patient, as montage changes during monitoring were frequent in the CHB-MIT database. Thus, only the EEG channels that are available throughout the entire duration of each patient's records are selected for further analysis, to ensure balanced data input and unbiased spectrum extraction, despite clinicians' decision to periodically add or remove EEG channels. Following the EEG recordings segmentation scheme of the database (i.e. each file contains one hour of digitized EEG signals, with only few having two and four hours long), the analysis is performed is epochs with a maximum duration of one hour. In cases where EEG records contained longer recordings, those were divided into smaller 1-h long epochs, accordingly.

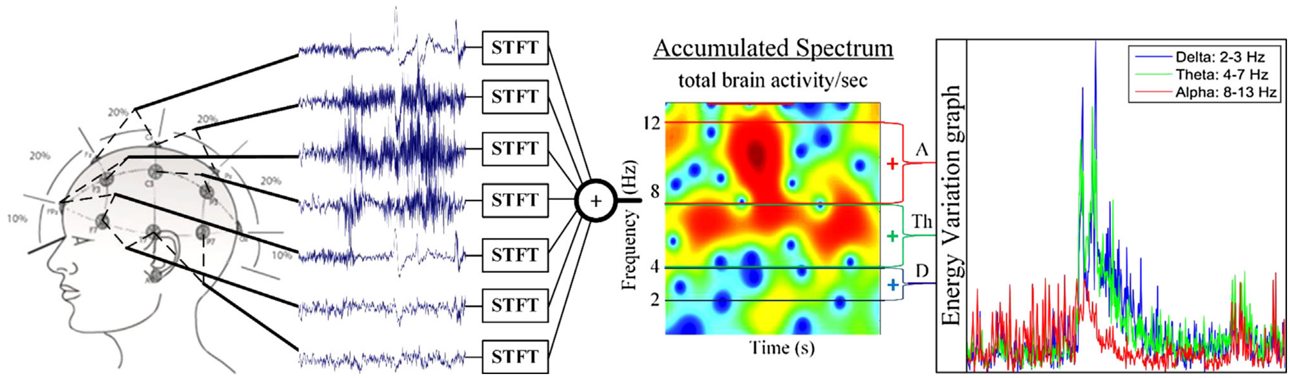

Fig. 1. Schematic representation of EEG analysis. EEG signal energy is extracted using STFT from every channel and summed to produce the Accumulated Spectrum. The brain's total energy distribution over, and bands is then estimated.

The STFT is directly applied to the selected channels without applying any signal preprocessing (i.e. filtering, artifact rejection, etc.) and the frequency contents of the EEG signals are extracted in small, consecutive segments using a sliding window. The length of the window is set to 1 s, with zero overlapping between subsequent segments, providing a maximum energy estimation of 128 Hz, given the signal's 256 Hz sampling frequency. The spectrum for the entire volume of the available EEG recordings per patient is extracted for every 1-h epoch in order to obtain the energy distribution of the EEG signals. Once the EEG spectrum of every channel has been extracted, the corresponding energy contents per channel are summed to produce the final image of the total brain activity distribution per 1-h EEG epoch ("*Accumulated Spectrum*", Fig. 1). Considering each channel's spectrum as a 128 × 3600 matrix (i.e. 128 Hz, 3600 s), the accumulated spectrogram *AC* is essentially the respective cell-by-cell sum (i.e. energy per Hz and second) of every channel:

$$AC(i,j) = \sum_{n=1}^{N} C_n(i,j), \tag{1}$$

where C_n is the EEG spectrum from the respective channel, N is the number of channels, $i = 2, 3, \ldots, 13$ is the frequency range in Hz (covering the delta, theta and alpha bands) and $j = 1, 2, \ldots, L$ is the length of the examined EEG epoch in seconds. In this way, each channel provides its share of spectral information to accurately estimate the distribution of the total brain activity per second of EEG signals.

Having acquired the total spectrum of the analyzed 1-h epoch, the final step is to isolate the energy contents of the delta (δ), theta (θ) and alpha (α) frequency bands. Each one of the three rhythms spans over a specific frequency range (i.e. $\delta \in$ 2–3 Hz, $\theta \in$ 4–7 Hz and $\alpha \in$ 8–13 Hz). However, in the proposed conditions the three EEG bands are considered as one-dimensional time series. Thus, their respective frequency values are summed to produce a single value representing the entire energy of each band per 1-s segment of EEG signals overall:

$$\delta = \sum_{i=2}^{3} AC(i,j) = \left[\delta_1, \delta_2, \delta_3, \ldots \delta_L\right], \tag{2}$$

$$\theta = \sum_{i=4}^{7} AC(i,j) = \left[\theta_1, \theta_2, \theta_3, \ldots \theta_L\right], \tag{3}$$

$$\alpha = \sum_{i=8}^{13} AC(i,j) = \left[a_1, a_2, a_3, \ldots a_L\right]. \tag{4}$$

The formulation of the above three time series from the analyzed EEG epoch provides an easy way to directly apply our seizure detection conditions. As shown in Fig. 1, the proposed methodology inputs the buffered 1-h long EEG data and outputs the δ, θ and α time series, providing an approximation of patient's brain total EEG activity over the three bands per second. In this way, a high rhythmical activity within any of the three frequency bands is expected to be detectable as its values will be significantly increased compared to the other two for that time instance. As mentioned before, such temporal variations in total EEG signal energy distribution among these frequency bands are expected due to seizure occurrence and are detected by the proposed methodology.

A typical graph of the extracted δ, θ and α fluctuations is presented in Fig. 2A. The graph depicts the actual distribution of EEG activity over the three bands for EEG data obtained from the first case of the CHB-MIT database (i.e. EEG record "chb01_04.edf"), including a seizure event. The patient's annotation file declares that the seizure begins at 1467 s and lasts for 28 s. As it is shown in Fig. 2A, the three bands are tightly coupled during inter-ictal and pre-ictal time intervals and the prevalence among them is constantly changing, with αband having a slight edge. This tightly coupled behavior is completely altered shortly after the marked seizure onset and for as long as the seizure evolves. The seizure interval is magnified in Fig. 2B, where it can be clearly seen that θ and δ activity is significantly higher than α, activating *Condition 4*. In addition, smaller short-lasting picks of θ band increments can be noted at the beginning and during the seizure, activating *Condition 1* which is also able to detect this seizure. Consequently, this particular seizure contains mainly four segments of interest, activating sequentially *Conditions 1, 4, 1* and *4* again. This seizure-oriented increase in both δ and θ bands energy is then gradually decreasing, with the frequency bands system returning to its normal tightly coupled state about two minutes after passing the marked seizure ending.

Depending on the activated condition, the area between the corresponding bands is estimated to quantify the concentration of EEG signal energy. For the seizure in Fig. 2B for example, when *Condition 4* is active, the area between the δ (blue) or θ (green) lines (i.e. depending on which is lower) and the α (red) line is the area of interest. This area is estimated using the trapezoidal rule for as long the seizure detection condition stays active:

$$\int_{t_1}^{t_2} [f_1(x) - f_2(x)]\, dx \approx \frac{1}{2}(t_2 - t_1)\,[f_1(t_1) - f_2(t_2) + f_1(t_2) - f_2(t_2)] \tag{5}$$

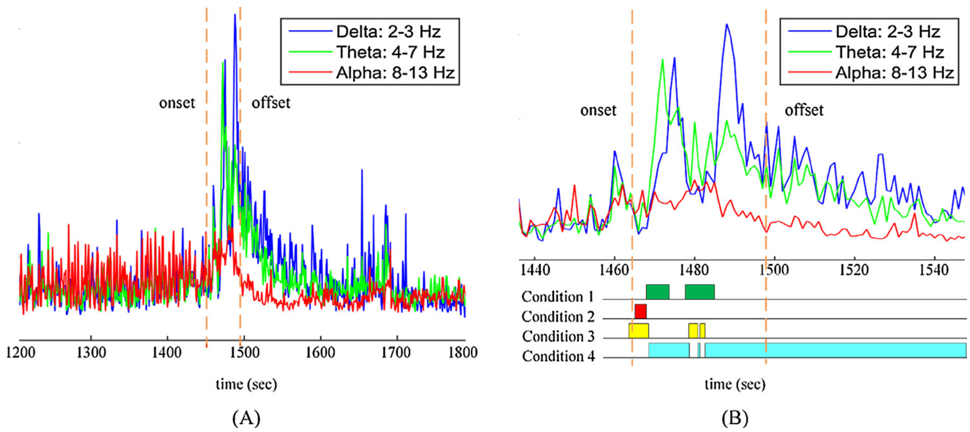

Fig. 2. (A) Energy distribution among, and bands of an actual EEG recording containing a seizure ("Chb01_04"). (B) Seizure detection conditions activation graph due to ictal activity. Seizure onset and offset time is marked with dashed lines.

where $f(x)$ is any of the δ, θ and αtime series (depending on the activated condition) and t_1, t_2 are the time intervals in which the condition remains active. The estimated area of each condition is used to rank the EEG segments. The larger the area, the larger the concentration of EEG activity and, thus, the more probable is for that particular EEG segment to contain ictal activity. Since normal rhythmical activity during the inter-ictal state could also be enough to trigger the activation of any of the four conditions, the key to effective seizure detection is to select EEG segments according to the area estimation of Eq. (5) from larger to smaller, expecting that seizure segments will be higher ranked in this scale. The best method for selecting the final set of segments that will be presented to the clinician for inspection is examined in the following section.

2.5. EEG segment selection

The total duration of EEG segments for visual inspection can be defined by the clinician or set at a default value, depending on the annotation requirements for each patient. Our aim is to demonstrate the robustness of the proposed methodology by achieving a high seizure detection rate at the range of 90%, with the least effort possible to speed-up the annotation process. The results of our preliminary study [43] suggested that setting this value at 5% (i.e. automatically discarding 95% of the available EEG recordings) is sufficient to produce 88% sensitivity on average, making it a good tradeoff between high seizure detection performance and low visual inspection time. Similar values for 3% and 7% of the total EEG data are also tested in this work. The duration of each selected EEG segment is equally important and needs to be long enough to allow the medical expert to reach an informed decision on whether it contains ictal activity or not. Thus, each segment must have a minimum duration of 15 s in order to ensure that accurate visual confirmation is feasible. This particular length is suggested as adequate by our medical experts. Segments of smaller duration are automatically extended to the minimum 15 s, while larger segments are retained to their initial length.

In order to provide a complete evaluation of the proposed unsupervised methodology and the best seizure detection performance estimation, four different segment selection methods are proposed in this section. In the first segment selection method, SSM I, the full length of the available EEG recordings per patient (i.e. 19–156 h, Table 1) is split and analyzed in 1-h epochs following the proposed methodology. From each 1-h long EEG epoch, an independent subset of potential seizure segments is extracted. For example, a 24-h long EEG recording will produce 24 subsets of candidate seizure segments, one set per hour. All these subsets of segments are grouped together into a single group and, then, they are sorted from larger to smaller, according to the area estimated using Eq. (5). Starting from the EEG segment with the largest area, segments are chosen for visual inspection until the maximum visual inspection time is reached. This method will demonstrate if ictal activity causes indeed the highest concentration of energy in any of the three frequency bands, compared to similar normal rhythmical activity, as seizure segments would occupy the top ranked positions.

In the second segment selection method, SSM II, the full length of the available EEG recordings per patient is split and analyzed again in 1-h epochs producing the same set of candidate seizure segments as above. However, in SSM II the EEG segments are selected from each one of the four seizure detection conditions independently, acquiring the top 25% of the segments from each condition, respectively. In this way, the total visual inspection time is divided equally among the four conditions, ensuring that all of them will contribute exactly the same to the final set of selected segments. This method should show a performance advantage if seizure-related EEG activity is dominant within the corresponding frequency band that better detects it, even if the rest of the EEG spectrum contains intense normal activity or it is extensively contaminated with noise and artifacts.

In the last two methods, SSM III and IV, the impact of temporal locality in seizure detection performance is investigated. In contrast to SSM I and II, in SSM III and IV the EEG segments that are more likely to contain ictal activity are independently selected as each 1-h long epoch is analyzed, unaffected by the signal's behavior in the rest of the patient's recordings. Thus, the most dominant rhythmical activity within each epoch is selected, instead of the most dominant activity overall, as in SSM I and II before. The total duration of selected segments is proportionally divided in each epoch (i.e. 5% per epoch, or 3 min/hr). Thus, the best EEG segments from every 1-h epoch will be included in the final set of EEG segments for visual inspection. The main advantage of SSM III and IV is that ictal activity needs to be prevalent only within the specific 1-h epoch that contains it and not over the entire length of recordings, making it easier to be detectable even if extensive noise and artifacts are present in other parts of the recordings. In SSM III, the EEG segments with the largest measured area per 1-h epoch are selected following the logic of SSM I (i.e. segments from every condition are grouped together and the ones with the largest area are selected). Finally, in SSM IV the duration of EEG segments per 1-h epoch is equally divided across the four seizure detection conditions as in SSM II (i.e. selecting the top 25% of segments per condition). SSM IV is the method with the most equal distribution of segment selection across both the four conditions and the available hours of EEG recordings per patient.

3. Results

The proposed unsupervised methodology is evaluated using the entire volume of the CHB-MIT EEG database. As no training samples are required, every EEG record per patient is analyzed following the steps described in Section 2.4 to obtain potential seizure segments (i.e. testing with 23 patients, 24 cases, 980 h of EEG recordings, 3,526,327 1-s long samples). Only three files from case 12 are excluded due to their radically changed montage half way during the patient's monitoring. Three values of total visual inspection time, set at 3%, 5% and 7% of each patient's total EEG recordings, are tested in three different evaluation experiments. These values demonstrate the enhancements of the proposed methodology in the time and effort required for the annotation of large EEG databases, as 97%, 95% and 93% of the total EEG data per patient, is automatically rejected as non-ictal, respectively. To evaluate the seizure detection performance, the EEG segments that are automatically selected as the most likely to contain ictal activity per patient, are validated using the annotation files provided in the CHB-MIT database. The validation shows that the majority of the seizures are successfully detected. The results are presented in full detail in Table 2.

SSM I showed a mean sensitivity of 57%, 69% and 73% and a false positives rate (FP) of 3.1 FP/h, 5.8 FP/h and 8.4 FP/h across all 24 cases for 3%, 5% and 7% of total visual inspection values, respectively. Balancing the inspection time across the four seizure detection conditions in SSM II resulted in an improved mean sensitivity of 76%, 80% and 83% for the same 3%, 5% and 7% values. The FP rates reached 4.4 FP/h, 7.3 FP/h and 10.5 FP/h, respectively. The temporal locality factor in segment selection, which is taken into account in SSM III and IV, has a positive impact on seizure detection performance. SSM III resulted in 64%, 69% and 74% mean sensitivity, which is slightly improved compared to SSM I, and 3.9 FP/h, 7.4 FP/h and 10.6 FP/h on average, respectively. Finally, the even allocation of segment selection across the four detection conditions and every EEG epoch provided the best results, as SSM IV scored the highest seizure detection performance, identifying up to 166 of the 185 seizures in total, with mean sensitivity 84%, 88% and 92%, for 3%, 5% and 7% visual inspection values, respectively. The false detection rate in this case reached 4.9 FP/h, 8.1 FP/h and 12.9 FP/h, respectively. Opting for STFT algorithm to extract the EEG spectrum, the computational cost of the proposed methodology is minimal, requiring less than 4 s to isolate potential seizure segments in a 1-h long EEG epoch using a typical i7 processor.

Besides seizure detection performance, we also wanted to evaluate the significance of each condition in detecting seizures. The impact of each condition is evaluated by measuring their contribution in terms of true positives or EEG segments that are correctly selected as ictal. The results are shown in Fig. 3. In total, *Condition 1* is proven to be the most relevant and, thus, θ band the most seizure-related frequency range in this group of patients, as 43% of the ictal segments present concentration of EEG activity in the θ band. The number of true positives is almost double to the equivalent of the second in order *Condition 4*, which accounted for 22% of the total ictal segments. Intense αband activity during seizures, which is captured by *Condition 2*, is also close with 19% of the total seizure segments, while *Condition 3* contributed the least true positives with 15%.

The possibility of improving seizure detection performance by using a subset of the proposed seizure detection conditions instead of all four is also investigated, by evaluating every possible combination of the four seizure detection conditions and seizure selection methods (SSM I–IV). The respective results are presented in Fig. 4. The significance of θ band/*Condition 1* in seizure detection is clearly depicted again, as it offers 74–75% sensitivity across all four SSMs on its own, while there is no highly ranked combination that does not include it as well. Following a more equal distribution of segment selection across the conditions and epochs (i.e. moving from the top left corner to the right and bottom of Fig. 4) resulted in an increased average of mean sensitivity of every combination from 61.93% in SSM I to 74.33% in SSM IV. Finally, using only *Conditions 1* and *2* and the SSM IV method, resulted in an 86% mean sensitivity across the 24 cases (149/185 seizures detected), thus, producing a notable seizure detection performance considering the even far more simplistic seizure detection model with only two conditions.

4. Discussion

The proposed unsupervised methodology for seizure detection shows great potential in identifying EEG segments where seizure-related activity is expressed without requiring *apriori* knowledge of the EEG dataset or complex signal processing techniques. The evaluation with the CHB-MIT EEG database revealed that the annotation time can be significantly reduced if the medical expert inspected only the selected segments, instead of manually scrolling throughout the entire duration of each patient's EEG recordings. The simplicity of the proposed seizure detection conditions, in regard to the high seizure detection performance obtained, is the greatest asset of this work, as they are patient-independent and not specifically designed for a certain epileptic syndrome or type of seizures. When 97%, 95% and 93% of each patient's EEG recordings are automatically rejected, 84%, 88% and 92% of each patient's seizures are successfully detected, on average, across the 24 cases of the CHB-MIT EEG database. In addition, as shown in Table 2, the proposed methodology is capable of detecting at least one seizure per patient in all of the 24 cases of the database, even for the lower 3% visual inspection ratio and at least half of each patient's seizures for 7% and using SSM IV. This is a solid indication of robustness, which is vital in order for such unsupervised methodologies to be accepted and gain applicability in everyday clinical practice.

As expected the segment selection process has a significant impact on seizure detection performance, since the preceding EEG analysis process is always the same. The four segment selection methods that are tested, SSM I–IV, demonstrate interesting facts about EEG behavior for both ictal and inter-ictal segments. Comparing the average seizure detection performance of SSM II to SSM I in Table 2, the mean sensitivity shows an increase of +13.34% (i.e. 79.67% vs 66.33%, respectively; average of 3%, 5% and 7% mean sensitivity), while the comparison of the equivalent SSM IV results to SSM III shows an even higher increase of +19% (i.e. 88% vs 69%, respectively; average of 3%, 5% and 7% mean sensitivity). This finding indicates that ictal EEG segments are ranked in top positions inside the particular group of the detection condition, which best fit their manifestation, causing indeed notable accumulation of signal energy over the examined frequency bands. However, this particular band is not necessarily more dominant compared to the others and ictal EEG activity is not always the most dominant rhythmical activity to be detected overall either.

Furthermore, the seizure detection performance improvement of SSM III compared to SSM I (i.e. +2.67%; 69% vs 66.33%, respectively) and more clearly that of SSM IV compared to SSM II (i.e. +8.33%; 88.00% vs 79.67%, respectively), suggests that temporal distribution of the selection of segments over the entire time of EEG recordings benefits performance as well. Considering that seizures are in general infrequent events, meaning that most of the 1-h long EEG epochs analyzed will most likely not contain epileptic activ-

Table 2
Evaluation results with the CHB-MIT EEG database. Results for all segment selection methods, SSM I, II, III and IV, are reported for 3%, 5% and 7% inspection values. Mean sensitivity denotes the average across all 24 cases.

Dataset info			SSM I			SSM II			SSM III			SSM IV		
Case	Time (hours)	# of seizures	3%	5%	7%	3%	5%	7%	3%	5%	7%	3%	5%	7%
1	40.5	7	5 (71%)	7 (100%)	7 (100%)	6 (86%)	7 (100%)	7 (100%)	5 (71%)	5 (71%)	5 (71%)	6 (86%)	6 (86%)	7 (100%)
2	35	3	2 (67%)	2 (67%)	3 (100%)	3 (100%)	3 (100%)	3 (100%)	2 (67%)	2 (67%)	2 (67%)	3 (100%)	3 (100%)	3 (100%)
3	38	7	5 (71%)	7 (100%)	7 (100%)	7 (100%)	7 (100%)	7 (100%)	7 (100%)	7 (100%)	7 (100%)	7 (100%)	7 (100%)	7 (100%)
4	156	4	3 (75%)	4 (100%)	4 (100%)	4 (100%)	4 (100%)	4 (100%)	4 (100%)	4 (100%)	4 (100%)	4 (100%)	4 (100%)	4 (100%)
5	39	5	5 (100%)	5 (100%)	5 (100%)	5 (100%)	5 (100%)	5 (100%)	5 (100%)	5 (100%)	5 (100%)	5 (100%)	5 (100%)	5 (100%)
6	66.5	10	0	0	1 (10%)	0	0	1 (10%)	1 (10%)	2 (20%)	2 (20%)	2 (20%)	4 (40%)	7 (70%)
7	67	3	3 (100%)	3 (100%)	3 (100%)	3 (100%)	3 (100%)	3 (100%)	3 (100%)	3 (100%)	3 (100%)	3 (100%)	3 (100%)	3 (100%)
8	20	5	4 (80%)	5 (100%)	5 (100%)	5 (100%)	5 (100%)	5 (100%)	5 (100%)	5 (100%)	5 (100%)	5 (100%)	5 (100%)	5 (100%)
9	68	4	4 (100%)	4 (100%)	4 (100%)	4 (100%)	4 (100%)	4 (100%)	4 (100%)	4 (100%)	4 (100%)	4 (100%)	4 (100%)	4 (100%)
10	50	7	6 (86%)	6 (86%)	6 (86%)	7 (100%)	7 (100%)	7 (100%)	6 (86%)	6 (86%)	6 (86%)	7 (100%)	7 (100%)	7 (100%)
11	35	3	1 (33%)	2 (67%)	2 (67%)	3 (100%)	3 (100%)	3 (100%)	2 (67%)	2 (67%)	2 (67%)	3 (100%)	3 (100%)	3 (100%)
12	21*	27*	8 (30%)	12 (44%)	14 (52%)	21 (78%)	26 (96%)	26 (96%)	7 (26%)	13 (48%)	18 (67%)	19 (70%)	23 (85%)	25 (93%)
13	33	12	3 (25%)	5 (42%)	5 (42%)	4 (33%)	4 (33%)	5 (42%)	4 (33%)	5 (42%)	7 (58%)	6 (50%)	7 (58%)	8 (67%)
14	26	8	1 (13%)	2 (25%)	4 (50%)	8 (100%)	8 (100%)	8 (100%)	1 (13%)	1 (13%)	2 (25%)	7 (88%)	8 (100%)	8 (100%)
15	40	20	5 (25%)	9 (45%)	12 (60%)	16 (80%)	17 (85%)	17 (85%)	10 (50%)	11 (55%)	12 (60%)	18 (90%)	18 (90%)	19 (95%)
16	19	10	0	0	0	1 (10%)	3 (30%)	4 (40%)	1 (10%)	2 (20%)	2 (20%)	4 (40%)	5 (50%)	5 (50%)
17	21	3	2 (67%)	3 (100%)	3 (100%)	2 (67%)	3 (100%)	3 (100%)	2 (67%)	3 (100%)	3 (100%)	3 (100%)	3 (100%)	3 (100%)
18	35.5	6	5 (83%)	5 (83%)	5 (83%)	6 (100%)	6 (100%)	6 (100%)	4 (67%)	4 (67%)	4 (67%)	6 (100%)	6 (100%)	6 (100%)
19	30	3	3 (100%)	3 (100%)	3 (100%)	3 (100%)	3 (100%)	3 (100%)	3 (100%)	3 (100%)	3 (100%)	3 (100%)	3 (100%)	3 (100%)
20	27.5	8	0	0	1 (13%)	0	0	0	1 (13%)	2 (25%)	5 (63%)	6 (75%)	8 (100%)	8 (100%)
21	33	4	0	0	0	2 (50%)	2 (50%)	2 (50%)	0	1 (25%)	1 (25%)	2 (50%)	2 (50%)	3 (75%)
22	31	3	3 (100%)	3 (100%)	3 (100%)	3 (100%)	3 (100%)	3 (100%)	3 (100%)	3 (100%)	3 (100%)	3 (100%)	3 (100%)	3 (100%)
23	26.5	7	3 (43%)	7 (100%)	7 (100%)	2 (29%)	3 (43%)	6 (86%)	4 (57%)	5 (71%)	6 (86%)	4 (57%)	4 (57%)	5 (71%)
24	21	16	14 (88%)	14 (88%)	14 (88%)	13 (81%)	14 (88%)	14 (88%)	14 (88%)	14 (88%)	14 (88%)	14 (88%)	14 (88%)	15 (94%)
Total:	~979	185	85/185,46%	108/185,58%	118/185,64%	128/185,69%	140/185,76%	146/185,79%	98/185,67%	112/185,61%	125/185,68%	144/185,78%	155/185,84%	166/185,90%
Mean Sensitivity:			57%	69%	73%	76%	80%	83%	64%	69%	74%	84%	88%	92%

* Files chb12_27-29 are rejected due to montage inconsistency with the rest of the patient's recordings.

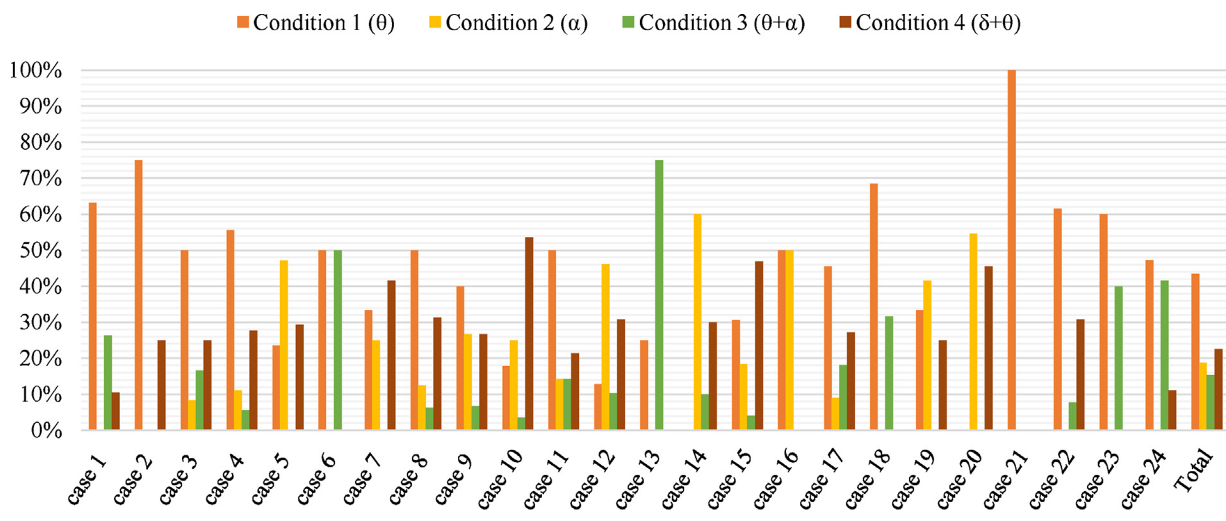

Fig. 3. Distribution of correctly identified seizure segments (True Positives), according to the Condition 1–4 they originated from.

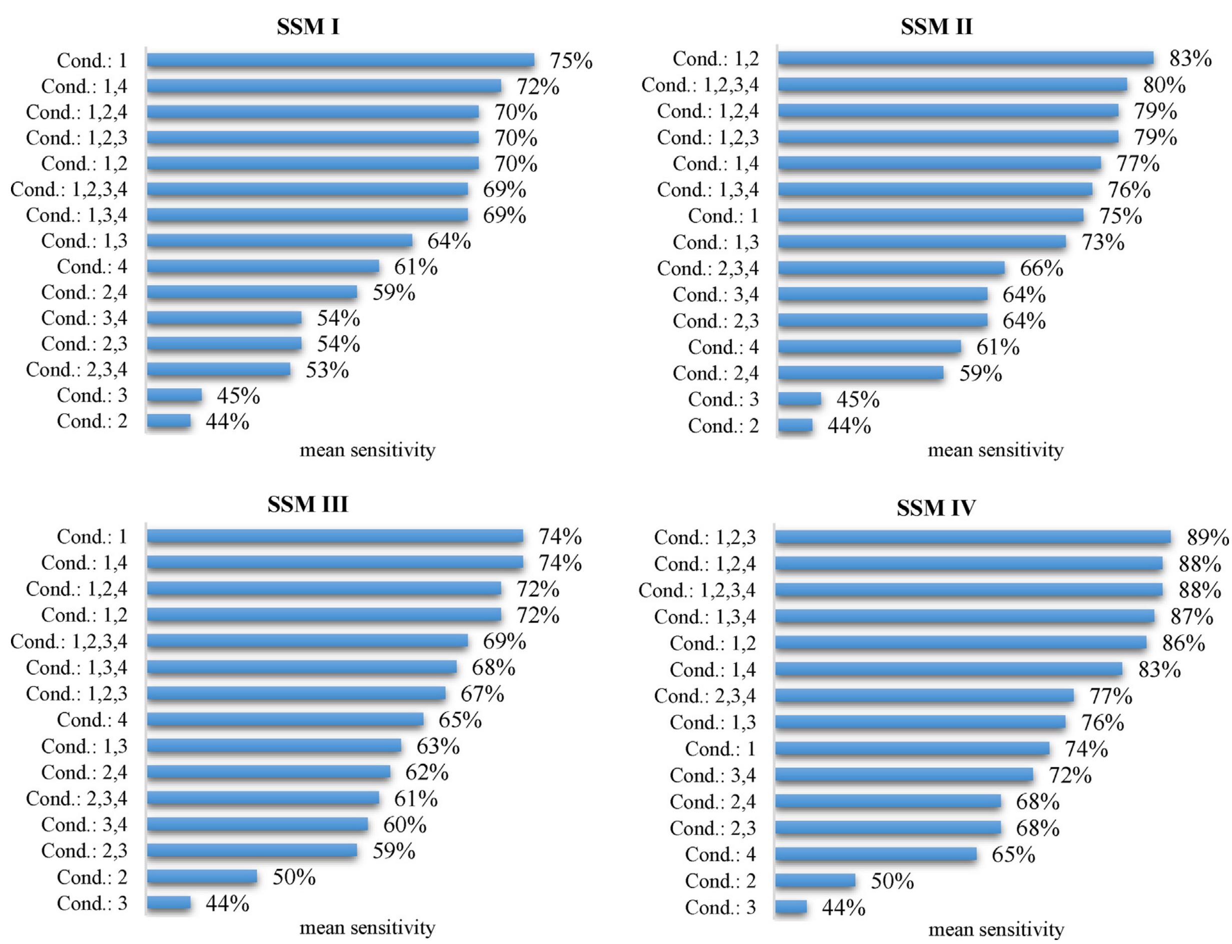

Fig. 4. Mean seizure detection Sensitivity for every possible combination of Conditions 1–4 and segment selection methods, SSM I-IV.

ity, this method could be considered as non-optimal. However, the better sensitivity results suggest that seizures are more easily detectable when they are compared to timely adjacent EEG data, as it is found to be easier to rank higher when competing only against the segments within the same 1-h epoch.

Regarding the contribution of each seizure detection condition, the evaluation shows that energy accumulation over the θ band (4–7 Hz) is the most seizure-relevant behavior among the 23 patients, being detected in 43% of the total ictal EEG segments (Fig. 3), while *Condition 1* also provided a high average sensitivity of 74% on its own (Fig. 4). On the other hand, *Condition 3* shows in general limited correlation to ictal activity and scored the lowest sensitivity on its own, suggesting that ictal activity extending in both θ and αbands (4–13 Hz) was rather uncommon in this group of patients. The results in Fig. 3 reveal a great variation in ictal EEG activity within the patients, as it can be seen that the contribution of each condition changes significantly from case to case. For example, despite being by far the most common in total, *Condition 1* does not

Table 3
Comparison with automated seizure detection methodologies available in the literature.

Reference	# of Patients	# of Seizures	Total EEG Duration	Methods	Training/ Evaluation/Dataset	Sensitivity	FD Rate
Birjandtalab et al. 2016 [25]	12	88	7 h	Power Spectral Density feature extraction, non-seizure/seizure data balance, clustering with Gaussian Mixture Model algorithm.	Balance of non-seizure/seizure data requires a priori knowledge of EEG. Subset of CHB-MIT EEG database.	80.3%*	98.3%*
Wilson et al., 2004 [17]	426	672	1049 h	Matching Pursuit, Neural Network and empirical rules for seizure detection, connected-object hierarchical clustering.	Pre-trained on selected exemplar seizures. False detection evaluation with non-epileptic EEG data. Own EEG dataset.	76%	0.11/h
Saab and Gotman, 2005 [15]	16	69	360 h	Wavelet decomposition, feature extraction, data segmentation, Bayes' formula estimates seizure/non-seizure probability of segments.	A priori probability estimation on exemplar EEG data (652 h, 126 seizures, 28 patients). Manual tuning to reduce FD. No seizures detected in 1 patient. Own EEG dataset.	76%	0.34/h
Mitra et al., 2009 [20]	76 (28 with seizures)	206	121 h	3-stage rulesets assessing: (1) potential seizure segments, (2) spatio-temporal clustering over multiple channels and (3) artifact rejection and seizure quality evaluation to reduce false detections.	Training set of 21 epileptic and 20 non-epileptic subjects. No seizures detected in 1 patient. Own EEG dataset.	79.8%	0.86/h
Kelly et al., 2010 [21]	55 (50 with seizures)	146	1200 h	EEG filtering, descriptor extraction frequency and amplitude variation, threshold-based artifact rejection and seizure activity criteria.	Training and threshold parameters adjustment on exemplar EEG data (3653 h, 141 seizures, 47 patient). No seizures detected in 4 patients. Own EEG dataset.	79.5%	0.09/h
Hopfengärtner et al., 2014 [22]	159	794	25278 h	Spectral analysis of selected electrodes, EEG energy in 2.5–12 Hz band referenced against multi-channel montages. Thresholding technique for seizure detection.	Threshold parameters adjusted on exemplar EEG data (19 patients). No seizures detected in 3 patients. Own EEG dataset.	87.3%	0.22/h
Mathieson et al., 2016 [18]	70 (35 with seizures)	2061	4060 h	Feature extraction, Support Vector Machine classifier, normalized (0–1) seizure probability output, corrected using Kalman filter. Threshold-based seizure detection.	Pre-trained on exemplar EEG data (268 h, 705 seizures, 19 patients). Manually set seizure probability threshold. No seizures detected in 2 patients. Own EEG dataset.	75%	0.4/h
Bogaarts et al., 2016 [19]	17 adults	1362	4018 h	Feature extraction, Support Vector Machine classifier, normalized seizure probability output, threshold-based seizure detection.	Training with 39 neonatal EEG recordings. 3 min of artefact- and seizure-free EEG manually selected in the beginning of each monitoring session. Own EEG dataset.	85.8% (AUC)	–
This work	23	185	980 h	Spectral analysis, variations in EEG energy distribution over delta, theta and alpha rhythms, simple rule-based seizure detection.	No training process involved. Evaluation with the entre CHB-MIT EEG database	88% (57% - 92%)	8.1/h (3.1/h – 12.9/h)

* Segment-based evaluation results

capture ictal activity in cases 14 and 20. That is probably due to the presence of different epileptic syndromes in these cases, but this is to be expected and must be taken into consideration for a robust unsupervised methodology. For this reason, the full set of seizure detection *Conditions 1–4* is preferred, as it could better deal with all the different types of epileptic activity that could be presented in clinical environment.

Table 3 presents the comparison with previous seizure detection methodologies. It should be noted that only Birjandtalab et al. [25] proposed an unsupervised methodology, whereas all the other researchers focused on supervised machine learning techniques, with the inherent limitation of requiring pre-annotated EEG recordings for training. However, since these methodologies were validated using out of sample EEG data, they are included as a reference even if direct comparison is not feasible. In the single unsupervised seizure detection work [25] that is available besides our preliminary analysis [42], the researchers proposed a Gaussian Mixture Model clustering methodology based on power spectral density features. Their methodology was evaluated with a small subset of the CHB-MIT EEG database using half of the patients available and only about 2 min of EEG signals before and after each seizure. The evaluation results were reported as segment-based analysis reaching 80.3% sensitivity and 98.3% specificity, respectively. Our methodology achieved higher sensitivity while using the entire volume of long-term EEG recordings rather than isolated segments.

As mentioned before, the rest of the articles are included, despite being supervised methodologies and using private EEG databases, to show exactly how challenging unsupervised seizure detection is. Compared to our work, the intermediate training step allowed optimizations that reduced the false detection rates, as supervised systems have awareness of factors that lead to false positives. In this way, the majority of the works in Table 3 reported significantly smaller FD rates than the proposed methodology. However, the proposed methodology has the advantage of not relying on the existence of pre-annotated EEG data, offering a considerable acceleration in the time and effort required for the annotation of large volumes of EEG data. Under this perspective, the increased false positive rate can be considered as a fair trade-off, which is further compensated by the greater sensitivity value that we obtained. In fact, our methodology resulted in the best measured sensitivity with 88% and only Hopfengärtner et al. [22] has reported a similar level of seizure detection performance.

Finally, it should be noted that five of the previous methodologies [15,18,20–22] failed to detect at least one seizure event for every subject involved in their corresponding evaluation datasets, while the proposed methodology did so even for the lower 3% visual inspection ratio and at least half of each patient's seizures for a 7% value. Failing to ensure that clinicians would always have at least one seizure to work with is why automated and particularly unsupervised systems are met with great skepticism from the medical personnel. In this regard, the proposed methodology has shown great robustness in its ability to accelerate the annotation of large volumes of continuous EEG recordings, proving that it can be effectively used in medical practice.

5. Conclusions

As long-term EEG monitoring of patients with epilepsy becomes increasingly popular in everyday practice the volume of EEG data requiring visual inspection will continue to grow as well. That is where the proposed unsupervised seizure detection methodology gains applicability as an annotation enhancement tool than can be used from medical experts to drastically reduce the time and effort required to examine large volumes of long-term EEG recordings. When only 5% of the EEG segments that are most likely to contain ictal activity are selected per patient, the proposed methodology reported 88% mean sensitivity across 24 cases with 8.1 FP/h on average, suggesting that the vast majority of the seizures can be successfully detected. This work demonstrates the benefits of designing EEG signal processing techniques with incorporated medical knowledge instead of focusing only on machine learning techniques.

References

[1] S. Noachtar, J. Rémi, The role of EEG in epilepsy: a critical review, Epilepsy Behav. 15 (2009) 22–33.

[2] L.J. Rodríguez-Sotelo, A. Osorio-Forero, A. Jiménez-Rodríguez, D. Cuesta-Frau, E. Cirugeda-Roldán, D. Peluffo, Automatic sleep stages classification using EEG entropy features and unsupervised pattern analysis techniques, Entropy 16 (2014).

[3] Maria Anastasiadou, Manolis Christodoulakis, S. Eleftherios Papathanasiou, S. Savvas, Papacostas Georgios, D. Mitsis, Unsupervised detection and removal of muscle artifacts from scalp EEG recordings using canonical correlation analysis, wavelets and random forests, clinical neurophysiology, Clin. Neurophysiol. (2017) 1388–2457, http://dx.doi.org/10.1016/j.clinph.2017.06.247 (Available online 8 July 2017, ISSN).

[4] H. Ren, J. Qu, Y. Chai, Q. Tang, Y. Zhou, An adaptive unsupervised classification of seizure method based on LMDMSSE with EEG signals, Biomed. Res. 28 (7) (2017).

[5] A. Subasi, J. Kevric, M.A. Canbaz, Epileptic seizure detection using hybrid machine learning methods, Neural Comput. Appl. 27 (April) (2017) 1–9, http://dx.doi.org/10.1007/s00521-017-3003-y (ISSN 1433–3058).

[6] K. Faraoun, A. Boukelif, Neural networks learning improvement using the K-means clustering algorithm to detect network intrusions, INFOCOMP J. Comput. Sci. 5 (2006) 28–36.

[7] U. Orhan, M. Hekim, M. Ozer, EEG signals classification using the K-means clustering and a multilayer perceptron neural network model, Expert Syst. Appl. 38 (2011) 13475–13481.

[8] W.G. Hofmann, M.P. Spreng, Unsupervised classification of EEG from subdural seizure recordings, Brain Topogr. 10 (1997) 121–132.

[9] L. Su, S. Zhiyi, S. Altay, A. Aydin, B. Nerse, A. Aviva, et al., Exploring the time–frequency content of high frequency oscillations for automated identification of seizure onset zone in epilepsy, J. Neural Eng. 13 (2016) 026026.

[10] J. Gotman, Automatic seizure detection: improvements and evaluation, Electroencephalogr. Clin. Neurophysiol. 76 (1990) 317–324.

[11] K. Schindler, H. Leung, C.E. Elger, K. Lehnertz, Assessing seizure dynamics by analysing the correlation structure of multichannel intracranial EEG, Brain 130 (2007) 65–77.

[12] W. Deburchgraeve, P.J. Cherian, M. De Vos, R.M. Swarte, J.H. Blok, G.H. Visser, et al., Automated neonatal seizure detection mimicking a human observer reading EEG, Clin. Neurophysiol. 119 (2008) 2447–2454.

[13] A. Garcés Correa, L. Orosco, P. Diez, E. Laciar, Automatic detection of epileptic seizures in long-term EEG records, Comput. Biol. Med. 57 (2015) 66–73.

[14] A. Aarabi, R. Fazel-Rezai, Y. Aghakhani, A fuzzy rule-based system for epileptic seizure detection in intracranial EEG, Clin. Neurophysiol. 120 (2009) 1648–1657.

[15] M.E. Saab, J. Gotman, A system to detect the onset of epileptic seizures in scalp EEG, Clin. Neurophysiol. 116 (2005) 427–442.

[16] Jesus Martinez-del-Rincon, Maria J. Santofimia, Jesus Barba Xavier del Toro, Francisca Romero, Patricia Navas, Juan C. Lopez, Non-linear classifiers applied to EEG analysis for epilepsy seizure detection, Expert Syst. Appl. 86 (2017) 99–112, http://dx.doi.org/10.1016/j.eswa.2017.05.052, 15 November 2017 ISSN 0957–4174.

[17] S.B. Wilson, M.L. Scheuer, R.G. Emerson, A.J. Gabor, Seizure detection: evaluation of the Reveal algorithm, Clin. Neurophysiol. 115 (2004) 2280–2291.

[18] S.R. Mathieson, N.J. Stevenson, E. Low, W.P. Marnane, J.M. Rennie, A. Temko, et al., Validation of an automated seizure detection algorithm for term neonates, Clin. Neurophysiol. 127 (2016) 156–168.

[19] J.G. Bogaarts, D.M.W. Hilkman, E.D. Gommer, V.H.J.M. van Kranen-Mastenbroek, J.P.H. Reulen, Improved epileptic seizure detection combining dynamic feature normalization with EEG novelty detection, Med. Biol. Eng. Comput. (2016) 1–10.

[20] J. Mitra, J.R. Glover, P.Y. Ktonas, A. Thitai Kumar, A. Mukherjee, N.B. Karayiannis, et al., A multi-stage system for the automated detection of epileptic seizures in neonatal EEG, journal of clinical neurophysiology, Off. Publ. Am. Electroencephalo-Graphic Soc. 26 (2009) 218–226.

[21] K.M. Kelly, D.S. Shiau, R.T. Kern, J.H. Chien, M.C.K. Yang, K.A. Yandora, et al., Assessment of a scalp EEG-based automated seizure detection system, Clin. Neurophysiol. 121 (2010) 1832–1843.

[22] R. Hopfengärtner, B.S. Kasper, W. Graf, S. Gollwitzer, G. Kreiselmeyer, H. Stefan, et al., Automatic seizure detection in long-term scalp EEG using an adaptive thresholding technique: a validation study for clinical routine, Clin. Neurophysiol. 125 (2014) 1346–1352.

[23] L. Wu, J. Gotman, Segmentation and classification of EEG during epileptic seizures, Electroencephalogr. Clin. Neurophysiol. 106 (1998) 344–356.
[24] O.L. Smart, N.H. Sephus, R.E. Gross, Application of modulation spectrum for iEEG seizure analysis, in Computational Intelligence in Bioinformatics and Computational Biology, 2014 IEEE Conference (2014) 1–8.
[25] J. Birjandtalab, M.B. Pouyan, M. Nourani, Unsupervised EEG analysis for automated epileptic seizure detection, First International Workshop on Pattern Recognition, International Society for Optics and Photonics (2016) (100110M-100110M-5).
[26] O. Smart, M. Chen, Semi-automated patient-specific scalp EEG seizure detection with unsupervised machine learning, Computational Intelligence in Bioinformatics and Computational Biology (CIBCB), 2015 IEEE Conference on (2015) 1–7.
[27] CHB-MIT Scalp EEG Database, 2017 ([Online]. Available at:) http://physionet.org/pn6/chbmit/.
[28] A.H. Shoeb, Application of Machine Learning to Epileptic Seizure Onset Detection and Treatment, Massachusetts Institute of Technology, 2009, 2017.
[29] A.L. Goldberger, L.A.N. Amaral, L. Glass, J.M. Hausdorff, P.C. Ivanov, R.G. Mark, et al., PhysioBank, PhysioToolkit, and PhysioNet: components of a new research resource for complex physiologic signals, Circulation 101 (2000) e215–e220.
[30] R.S. Fisher, W.V.E. Boas, W. Blume, C. Elger, P. Genton, P. Lee, J. Engel, Epileptic seizures and epilepsy: definitions proposed by the international league against epilepsy (ILAE) and the international bureau for epilepsy (IBE), Epilepsia 46 (4) (2005) 470–472.
[31] M.J. Doherty, Atlas of epilepsy, Arch. Neurol. 64 (4) (2007), 604–604.
[32] K.M. Tsiouris, A.T. Tzallas, S. Markoula, D. Koutsouris, S. Konitsiotis, D.I. Fotiadis, A review of automated methodologies for the detection of epileptic episodes using long-Term EEG signals, in: Handbook of Research on Trends in the Diagnosis and Treatment of Chronic Conditions, 2015, pp. 231.
[33] S. Smith, EEG in the diagnosis, classification, and management of patients with epilepsy, J. Neurol. Neurosurg. Psychiatry 76 (2005) ii2–ii7.
[34] R. Meier, H. Dittrich, A. Schulze-Bonhage, A. Aertsen, Detecting epileptic seizures in long-term human EEG: a new approach to automatic online and real-Time detection and classification of polymorphic seizure patterns, J. Clin. Neurophysiol. 25 (2008) 119–131.
[35] S. Noachtar, A.S. Peters, Semiology of epileptic seizures: a critical review, Epilepsy Behav. 15 (2009) 2–9.
[36] I. Osorio, H.P. Zaveri, M.G. Frei, S. Arthurs, Epilepsy: The Intersection of Neurosciences, Biology, Mathematics, Engineering, and Physics, CRC Press, 2016, 2017.
[37] K. Majumdar, Human scalp EEG processing: various soft computing approaches, Appl. Soft Comput. 11 (2011) 4433–4447.
[38] S. Nasehi, H. Pourghassem, Seizure detection algorithms based on analysis of EEG and ECG signals: a survey, Neurophysiology 44 (2012) 174–186.
[39] U.R. Acharya, S. Vinitha Sree, G. Swapna, R.J. Martis, J.S. Suri, Automated EEG analysis of epilepsy: a review, Knowledge-Based Syst. 45 (2013) 147–165.
[40] N.E. Huang, Z. Shen, S.R. Long, M.C. Wu, H.H. Shih, Q. Zheng, et al., The empirical mode decomposition and the Hilbert spectrum for nonlinear and non-stationary time series analysis, Proceedings of the Royal Society of London A: Mathematical, Physical and Engineering Sciences (1998) 903–995.
[41] M. Akay, Time frequency and wavelets in biomedical signal processing, IEEE Press Series in Biomedical Engineering (1998).
[42] K.M. Tsiouris, S. Konitsiotis, S. Markoula, D.D. Koutsouris, A.I. Sakellarios, D.I. Fotiadis, An unsupervised methodology for the detection of epileptic seizures in long-term EEG signals, in Bioinformatics and Bioengineering (BIBE), 2015 IEEE 15th International Conference on (2015) 1–4.